

A comparative study of Gaussian Graphical Model approaches for genomic data

P. F. Stifanelli,^{1,2} T. M. Creanza,^{1,3} R. Anglani,¹ V. C. Liuzzi,¹ S. Mukherjee,⁴ and N. Ancona¹

¹*Institute of Intelligent Systems for Automation, National Research Council – CNR, I-70126, Bari, Italy*

²*Physics Department, University of Bari, I-70126, Bari, Italy*

³*Department of Emergency and Organ Transplantation – DETO, University of Bari, I-70124, Bari, Italy*

⁴*Institute for Genome Sciences and Policy, Center for Interdisciplinary Engineering, Medicine and Applied Sciences, Duke University, 101 Science Drive, Durham, NC 27708, USA*

The inference of networks of dependencies by Gaussian Graphical models on high-throughput data is an open issue in modern molecular biology. In this paper we provide a comparative study of three methods to obtain small sample and high dimension estimates of partial correlation coefficients: the Moore-Penrose pseudoinverse (PINV), residual correlation (RCM) and covariance-regularized method (ℓ_{2C}). We first compare them on simulated datasets and we find that PINV is less stable in terms of AUC performance when the number of variables changes. The two regularized methods have comparable performances but ℓ_{2C} is much faster than RCM. Finally, we present the results of an application of ℓ_{2C} for the inference of a gene network for isoprenoid biosynthesis pathways in *Arabidopsis thaliana*.

INTRODUCTION

One of the aims of systems biology is to provide quantitative models for the study of complex interaction patterns among genes and their products that are the result of many biological processes in the cell, such as biochemical interactions and regulatory activities. In this framework, graphical models [1] have been exploited as useful stochastic tools to investigate and describe the conditional independence structure between random variables. In particular, the Graphical Gaussian Models (GGM) use the partial correlation estimates as a measure of conditional independence between any two variables [2]. Unfortunately, the application of GGMs classical theory is still a hard task. The genomic data are typically characterized by a huge number of genes p with respect to the small number of available samples n . This makes unreliable the application of the classical GGMs theory to the small sample setting case. In recent years, several methods have been proposed to overcome this problem by reducing the numbers of genes or gene lists in order to reach the $n > p$ regime [3]. Other solutions have been also proposed [4–6] to circumvent the problem of computing full partial correlation coefficients by using only zero and first order coefficients. However, these approaches do not take into account all multigene effects on each pair of variables. A more sophisticated way to adapt GGMs to the $n < p$ case is to find regularized estimates for the covariance matrix [7–9] and its inverse. Once regularized estimates of partial correlation are available, heuristic searches can be used to find an optimal graphical model. A fundamental assumption to perform these quantitative methods is the sparsity of biological networks: only a few edges are supposed to be present in the gene regulatory networks, so that reliable estimates of the graphical model can be inferred also in small sample case [5]. A regularized GGM method based on a Stein-type shrinkage has been applied to genomic data [10] and the network selection has been based on false discovery rate multiple testing. In Ref. [11] the same procedure to select the network has been adopted, with a Moore-Penrose pseudoinverse method to obtain the concentration matrix. Finally, the authors in Ref. [12] have suggested an attractive and simple approach based on lasso-type regression to select among the partial correlations the nonzero values, paving the way to a number of analysis and novel algorithms based on lasso ℓ_1 regularizations [7–9, 13]. In this work, we focus on regularized methods for the estimation of the concentration matrix in an undirected GGM. In particular, we present a comparative study of three methods in terms of AUC (area under the Receiving Operative Characteristic curve) and timing performances. One is based on Moore-Penrose pseudoinverse (PINV), the other two provide an estimate of the partial correlation coefficients, based on Regularized Least Square regression (RCM) and a covariance-regularized method with a ℓ_2 penalty in the log-likelihood function (ℓ_{2C}). Finally, we apply the ℓ_{2C} method to infer a gene network for the isoprenoid biosynthesis pathways in *A. thaliana*. This network structural analysis allows to enlight some expected pathway properties. In particular, we find a negative partial correlation coefficient between the two hubs in the two isoprenoid pathways. This suggests a different response of the pathways to the several tested experimental conditions and, together with the high connectivity of the two hubs, provides an evidence of cross-talk between genes in the plastidial and the cytosolic pathways.

GAUSSIAN NETWORKS FROM MICROARRAY DATA

Let $\mathbf{X} = (X_1, \dots, X_p) \in \mathbb{R}^p$ be a random vector distributed according a multivariate normal distribution $\mathcal{N}(\boldsymbol{\mu}, \boldsymbol{\Sigma})$. The interaction structure between these variables can be described by means of a graph $G = (V, E)$, where V is the vertex set and E is the edge set. If vertices of V are identified with the random variables X_1, \dots, X_p , then the edges of E can represent the conditional dependence between the vertices. In other words, the absence of an edge between the i -th and j -th vertex means a conditional

independence between the associated variables X_i and X_j . In this study, we shall consider only undirected Gaussian graphs G with *pairwise Markov property*, such that for all $(i, j) \notin E$ one has

$$X_i \perp\!\!\!\perp X_j \mid X_{V \setminus \{i, j\}} \quad i, j = 1, \dots, p, \quad (1)$$

i.e. X_i and X_j are conditionally independent being fixed all other variables $X_{V \setminus \{i, j\}}$. Since \mathbf{X} follows a p -variate normal distribution, the condition (1) turns out to be $\rho_{ij \cdot V \setminus \{i, j\}} = 0$, where $\rho_{ij \cdot V \setminus \{i, j\}}$ is the partial correlation coefficient between the i -th and j -th variable, being fixed all other variables. It has been shown [1] that partial correlation matrix elements are related to the *precision matrix* (or inverse covariance matrix) $\Theta = \Sigma^{-1}$, as:

$$\rho_{ij \cdot V \setminus \{i, j\}} = -\frac{\theta_{ij}}{\sqrt{\theta_{ii}\theta_{jj}}} \quad i \neq j, \quad (2)$$

where θ_{ij} are elements of Ω . In general, when the number of observations n is greater than the number of variables p , it is straightforward to evaluate θ_{ij} in Eq. (2) by inverting the sample covariance matrix. Unfortunately, a typical genomic dataset is characterized by $n < p$, so that the sample covariance matrix becomes not invertible [14]. For this reason, in order to estimate the partial correlation matrix one needs alternative methods to overcome the problem, like regularization methods, ridge regression or pseudoinverse.

Partial correlation matrix estimation

In order to describe the three methods that we shall investigate, let us consider the $n \times p$ matrix $\mathbf{X} = (\mathbf{X}_1, \mathbf{X}_2, \dots, \mathbf{X}_p)$, where each $\{\mathbf{X}_i\} \in \mathbb{R}^n$, with $n < p$. Let us indicate \mathbf{S} as the estimate of the covariance matrix Σ and $\hat{\Theta}$ as the estimate of inverse covariance matrix Σ^{-1} .

Pseudoinverse method (PINV)

The precision matrix $\hat{\Theta}$ can be obtained as pseudoinverse of \mathbf{S} , by using the Singular Value Decomposition (SVD). Indeed, a singular value decomposition of a $m \times q$ matrix M , is $M = U\Lambda V^*$, where U is a $m \times m$ unitary matrix, Λ is $m \times q$ diagonal matrix with nonnegative real numbers on the diagonal and V^* is a $q \times q$ unitary matrix (transpose conjugate of V). Then, the pseudoinverse of M is $M^+ = V\Lambda^+U^*$, where Λ^+ is obtained by replacing each diagonal element with its reciprocal and then transposing the matrix.

Covariance-regularized method (ℓ_2)

Let us consider a log likelihood function with a ℓ_2 penalization [9]:

$$L(\Theta) = \log \det \Theta - \text{Tr}(\mathbf{S}\Theta) - \lambda \|\Theta\|_F^2, \quad (3)$$

with $\lambda > 0$ and $\|\Theta\|_F^2 = \text{tr}(\Theta^\top \Theta)$. The maximization of Eq. (3) with respect to Θ is equivalent to solve the following equation

$$\hat{\Theta}^{-1} - 2\lambda \hat{\Theta} = \mathbf{S}. \quad (4)$$

Consequently, the problem turns out to be an eigenvalue problem, therefore the eigenvalues θ_i of $\hat{\Theta}$ can be evaluated as function of the eigenvalues s_i of \mathbf{S} :

$$\theta_i^\pm = -\frac{s_i}{4\lambda} \pm \frac{\sqrt{s_i^2 + 8\lambda}}{4\lambda}. \quad (5)$$

Since Θ must be positive definite, the correct value of θ_i is θ_i^+ then, for the spectral theorem the precision matrix $\hat{\Theta}$ is given by

$$\hat{\Theta} = \sum_{i=1}^{\ell} \theta_i^+ \mathbf{u}_i \mathbf{u}_i^\top. \quad (6)$$

Finally, in order to estimate the parameter λ that maximizes the penalized log-likelihood function in Eq. (3), we carry out 20 random splits of the data set in training and validation sets and then we evaluate the log-likelihood over the validation set.

n	ℓ_{2C}			PINV			RCM		
	AUC	AUC std	T (s)	AUC	AUC std	T (s)	AUC	AUC std	T (s)
r 500	0.998	0.0001	38.86	0.987	0.0006	0.161	0.999	0.0001	8343
h 500	1.000	0.0000	83.74	0.999	0.0000	0.164	1.000	0.0000	6468
c 500	0.995	0.0002	84.95	0.963	0.0014	0.164	0.996	0.0002	6449
r 200	0.976	0.0003	38.44	0.581	0.0161	0.111	0.984	0.0006	3566
h 200	1.000	0.0000	81.13	0.806	0.0150	0.115	0.999	0.0001	3555
c 200	0.936	0.0008	82.02	0.587	0.0049	0.121	0.923	0.0009	3747
r 20	0.808	0.0011	39.03	0.929	0.0018	0.093	0.924	0.0017	105
h 20	0.999	0.0001	82.03	1.000	0.0000	0.091	0.999	0.0000	106
c 20	0.668	0.0014	82.13	0.659	0.0014	0.091	0.659	0.0014	108

TABLE I: AUC, AUC standard error and timing performances for $p = 400$. *Left part:* ℓ_{2C} method. *Center part:* PINV. *Right part:* RCM. Indices r , h and c stand for random, hubs and clique pattern, respectively.

Residual correlation method (RCM)

We consider a regression model for the variables \mathbf{X}_i and \mathbf{X}_j as

$$\mathbf{X}_i = \langle \beta_{(i)}, \mathbf{X}_{\setminus i \setminus j} \rangle + b_i \quad \mathbf{X}_j = \langle \beta_{(j)}, \mathbf{X}_{\setminus i \setminus j} \rangle + b_j \quad (7)$$

where $\{\beta_{(i)}\}$ is the regression coefficient vector in $p - 2$ dimensions referred to the i -th gene; \mathbf{X}_i is the i -th column of the matrix \mathbf{X} and $\mathbf{X}_{\setminus i \setminus j}$ is \mathbf{X} without the i -th and j -th columns. The Regularized Least Square (RLS) [15] method evaluates the regression models (7) by solving

$$\min_{\beta \in \mathbb{R}^{p-2}} \frac{1}{n} \|\mathbf{X}_i - \beta_{(i)} \mathbf{X}_{\setminus i \setminus j}\|_2^2 + \lambda \|\beta_{(i)}\|_2^2. \quad (8)$$

Now, if $\tilde{\mathbf{X}}_i$ and $\tilde{\mathbf{X}}_j$ are the RLS estimates of \mathbf{X}_i and \mathbf{X}_j , one can evaluate the residual vectors $\mathbf{r}_i = \tilde{\mathbf{X}}_i - \mathbf{X}_i$ and $\mathbf{r}_j = \tilde{\mathbf{X}}_j - \mathbf{X}_j$. This allows to evaluate the partial correlation coefficients $\rho_{ij|p-2}$ between the i -th and j -th variable being fixed all other $p - 2$ variables as the Pearson correlation $r_{r_i r_j}$ between the residuals, i.e.

$$\rho_{ij|p-2} = r_{r_i r_j} = \frac{\text{cov}(\mathbf{r}_i, \mathbf{r}_j)}{\sqrt{\text{var}(\mathbf{r}_i) \cdot \text{var}(\mathbf{r}_j)}}. \quad (9)$$

Finally, the $\lambda > 0$ parameter has been chosen by minimizing the Leave-One-Out cross validation errors.

COMPARATIVE STUDY OF ACCURACY

Data generation

Datasets with different numbers of variables and observations have been used in order to investigate the performances of the methods, i.e. $p = \{50, 200, 400\}$ and $n = \{20, 200, 500\}$. Each dataset \mathbf{X} has been generated from a multivariate gaussian distribution with zero mean and covariance $\Sigma_{\text{th}} = \Theta_{\text{th}}^{-1}$. The structure of the precision matrix Θ_{th} presents the following patterns [13]: *random*, *hubs* and *cliques* and it has approximately p non vanishing entries out of the $p(p - 1)/2$ off-diagonal elements, except for clique configuration where the entries are approximately $2p$.

In the *random* pattern, the off-diagonal terms of Θ_{th} are set randomly to a fixed value $\theta \neq 0$. In the *hubs* configuration, we partition the columns into disjoint groups G_k , where index k indicates the k -th column chosen as “central” in each group. Then the off-diagonal terms are set $\theta_{ik} = \theta$ if $i \in G_k$, otherwise $\theta_{ik} = 0$. In the *cliques* pattern, the precision matrix is partitioned as done in *hubs* and the off-diagonal terms θ_{ij} are set to θ if $i, j \in G_k$, with $i \neq j$. The positive definiteness for each configuration, is guaranteed by the diagonal entries which are selected in order to keep Θ_{th} diagonally dominant.

n	ℓ_{2C}			PINV			RCM		
	AUC	AUC std	T (s)	AUC	AUC std	T (s)	AUC	AUC std	T (s)
<i>r</i> 500	0.999	0.0001	5.807	0.999	0.0001	0.0377	0.999	0.0001	807
<i>h</i> 500	1.000	0.0000	10.655	1.000	0.0000	0.0376	1.000	0.0000	450
<i>c</i> 500	0.996	0.0002	10.821	0.999	0.0001	0.0439	0.999	0.0000	436
<i>r</i> 200	0.986	0.0003	5.592	0.703	0.0067	0.0310	0.990	0.0007	861
<i>h</i> 200	1.000	0.0000	10.425	0.748	0.0124	0.0309	0.999	0.0003	856
<i>c</i> 200	0.944	0.0010	10.529	0.612	0.0064	0.0336	0.950	0.0008	1028
<i>r</i> 20	0.784	0.0016	6.150	0.880	0.0048	0.0187	0.871	0.0046	24.5
<i>h</i> 20	0.999	0.0001	10.574	0.999	0.0002	0.0182	0.999	0.0001	27.9
<i>c</i> 20	0.669	0.0016	10.545	0.649	0.0017	0.0189	0.654	0.0017	25.3

TABLE II: AUC, AUC standard error and timing performances for $p = 200$. *Left part:* ℓ_{2C} method. *Center part:* PINV. *Right part:* RCM. Indices r , h and c stand for random, hubs and clique pattern, respectively.

Performances

In order to compare the performances of the three methods, we have used this procedure: (I) For each data generation pattern, draw a random dataset \mathbf{X} from $\mathcal{N}(\mathbf{0}, \Sigma_{th})$; (II) Evaluate \mathbf{S} and Θ_{exp} in the case of PINV and ℓ_{2C} , hence find ρ_{exp} from Eq. (2); in the case of RCM use Eq. (9) for the evaluation of ρ_{exp} ; (III) For each method, evaluate the AUC performance, as follows. Since the edges in our simulated dataset have the same strength and we know the label edge and non edge for each element, the elements of ρ_{exp} can be divided in two sets: ρ_{exp} for the edge elements and ρ_{exp} for the non edge ones. The AUC measures the performances of the three methods in terms of accuracy of classification of edge and non edges by using the relative ρ_{exp} values.

RESULTS

In Tables I, II and III we present the AUC, AUC standard error and timing (in seconds) performances for $p = \{400, 200, 50\}$, respectively. Each table is divided in three columns related to the analyzed methods. Indices r , h , and c refer to the three data generation methods: random, hubs, and clique. The results shown are averaged over 20 trials for $n = \{500, 200, 20\}$.

As expected, when $n > p$ all methods provide the same efficiency with an AUC virtually equal to 1. In fact, in this case the use of regularization methods should be not required. When $p > n$, we find that PINV presents some instability in AUC outcomes, mainly in those region when $p \approx n$. This can be due to a “resonance effect”, as explained in Refs. [11, 16]. Instead, RCM and ℓ_{2C} show high value of AUC in all settings and have similar performances, almost independently of the range of p and n . Note that, only in the random configuration, when $n = 20$ and $p = \{200, 400\}$, RCM shows AUC values 10% larger than ℓ_{2C} ones. On the other hand, the timing comparison highlights that ℓ_{2C} is much faster than the RLS-based method.

APPLICATION TO BIOLOGICAL PATHWAYS

Isoprenoids play various important roles in plants, functioning as membrane components, photosynthetic pigments, hormones and plant defence compounds. They are synthesized through condensation of the five-carbon intermediates isopentenyl diphosphate (IPP) and dimethylallyl diphosphate (DMAPP). In higher plants, IPP and DMAPP are synthesized through two different routes that take place in two distinct cellular compartments. The cytosolic pathway, also called MVA (mevalonate) pathway, provides the precursors for sterols, ubiquinone and sesquiterpenes [17]. An alternative pathway, called MEP/DOXP (2-C-methyl-D-erythritol 4-phosphate / 1-deoxy-D-xylulose 5-phosphate), is located in the chloroplast and is used for the synthesis of isoprene, carotenoids, abscisic acid, chlorophylls and plastoquinone [18]. Although this subcellular compartmentation allows both pathways to operate independently, there are several evidences that they can interact in some conditions [19]. Inhibition of the MVA pathway in *A. thaliana* leads to an increase of carotenoids and chlorophylls levels, demonstrating that its decreased functioning can be partially compensated for by the MEP/DOXP pathway. Inversely, inhibition of the MEP/DOXP pathway in seedlings causes the reduction of levels in carotenoids and chlorophylls, indicating a unidirectional transport of isoprenoid intermediates from the chloroplast to the cytosol. In order to investigate whether the transcriptional regulation is at the basis of the crosstalk between the cytosolic and the plastidial pathways, Laule et al. [19] have studied this interaction by identifying

n	ℓ_{2C}			PINV			RCM		
	AUC	AUC std	T (s)	AUC	AUC std	T (s)	AUC	AUC std	T (s)
<i>r</i> 500	0.999	0.0000	0.4401	1.000	0.0000	0.0152	1.000	0.0000	2.76
<i>h</i> 500	1.000	0.0000	0.4506	1.000	0.0000	0.0061	1.000	0.0000	4.19
<i>c</i> 500	0.999	0.0000	0.4184	1.000	0.0000	0.0065	1.000	0.0000	3.45
<i>r</i> 200	0.996	0.0004	0.4206	0.997	0.0004	0.0038	0.998	0.0004	1.92
<i>h</i> 200	1.000	0.0000	0.4266	1.000	0.0000	0.0030	1.000	0.0000	2.26
<i>c</i> 200	0.976	0.0023	0.3971	0.985	0.0009	0.0036	0.978	0.0011	2.10
<i>r</i> 20	0.821	0.0047	0.4106	0.654	0.0097	0.0024	0.815	0.0066	1.56
<i>h</i> 20	1.000	0.0000	0.4174	0.542	0.0076	0.0019	0.866	0.0081	1.43
<i>c</i> 20	0.675	0.0052	0.3776	0.574	0.0076	0.0022	0.666	0.0057	1.48

TABLE III: AUC, AUC standard error and timing performances for $p = 50$. *Left part:* ℓ_{2C} method. *Center part:* PINV. *Right part:* RCM. Indices r , h and c stand for random, hubs and clique pattern, respectively.

the genes with expression levels changed as a response to the inhibition. They have shown that the inhibitor mediated changes in metabolite levels are not reflected in changes in gene expression levels, suggesting that alterations in the flux through the two isoprenoid pathways are not transcriptionally regulated. In order to clarify the interaction between both pathways at the transcriptional level, Wille et al. [4] have explored the structural relationship between genes on the basis of their expression levels under different experimental conditions. This study aims to infer the regulatory network of the genes in the isoprenoid pathways by incorporating the expression levels of 795 genes from other 56 metabolic pathways. Moving beyond the one-gene approach, the authors have found various connections between genes in the two different pathways, suggesting the existence of a crosstalk at the transcriptional level.

Results from the covariance-regularized method for *A. thaliana* isoprenoid pathways

We apply the ℓ_{2C} method to the publicly available data set from Ref. [4]. The selection of the graph is performed by computing the 95% bootstrap confidence interval of the statistics and the absence of an edge occurs when the zero is included in this interval. The data consist of expression measurements for 39 genes in the isoprenoid pathways and 795 in other 56 pathways assayed on 118 Affymetrix GeneChip microarrays. We are interested in the construction of a gene network in the two isoprenoid pathways in order to detect the effects of genes in the other pathways. In Fig. 1 we reproduce the inferred network with 44 edges. For each pathway we find a module with strongly interconnected and positively correlated genes. This suggests the reliability of our method since genes within the same pathway are potentially jointly regulated [20]. Furthermore, we identify two strong candidate genes for the cross-talk between the pathways: HMGS and HDS. HMGS represents the hub of the cytosolic module, because it is positively correlated to five genes of the same pathway: DPPS1, MDPC1, AACT2, HMGR2 and MK. It encodes a protein with hydroxymethylglutaryl-CoA synthase activity that catalyzes the second step of the MVA pathway. HDS represents the hub of the plastidial module, because it is positively correlated to five genes of the same pathway: DXPS1, MECPS, GGPPS12, IPP11 and PPDS2. It encodes a chloroplast-localized hydroxy-2-methyl-2-(E)-butenyl 4-diphosphate synthase and catalyzes the penultimate step of the biosynthesis of IPP and DMAPP via the MEP/DOXP pathway. The negative correlation between HMGS and HDS means that they respond differently to the several tested experimental conditions. This, together with the high connectivity of the two hubs, provides an evidence of cross-talk between genes in the plastidial and the cytosolic pathways. Other negative correlations between the two pathways are represented by the edges HMGR2–MECPS, MPDC2–PPDS2 and MPDC2–DXPS2. Interestingly, the plastidial gene IPP11 is found to be positively correlated to the module of connected genes in the MVA pathway (IPP11–MK, IPP1–IPP12). This evidence confirms the results of Ref. [6] where they guess that the enzyme IPP11 controls the steady-state levels of IPP and DMAPP in the plastid, when a high level of transfer of intermediates between plastid and cytosol takes place. Moreover, our study shows three candidate mitochondrial genes for the cross-talk (DPPS2, GGPPS5 and UPPS1) which are in the plastidial module. Finally, it is interesting to note that the method used in Ref. [4] includes more cross-links between the two pathways with respect to the ℓ_{2C} method. Although from the literature it is known the existence of an interaction between the two pathways, we believe that this cross-link should not be so strong, as genes of the two pathways belong to two different cell compartments. A possible explanation of such a difference is that Wille *et al.* construct a network based on the first-order conditional dependence that may not capture multi-gene effects on a given pair of genes.

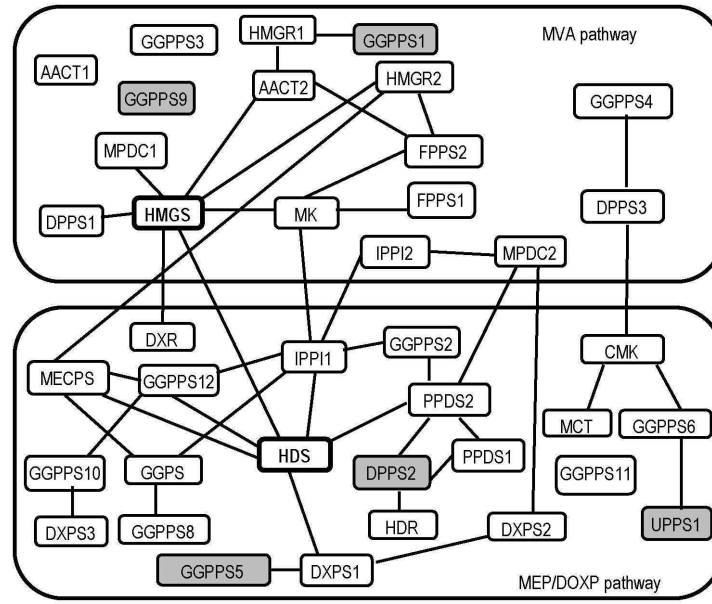


FIG. 1: Biological network of the isoprenoid pathways inferred by using PLLM. *Upper part*: Genes of MVA pathway. *Lower part*: Genes of MEP/DOXP pathway. Grey boxes refer to mitochondrial genes; HMGS and HDS represent the hubs of the two modules.

CONCLUSIONS

In this paper, we present a comparative study of three different methods to infer networks of dependencies by estimates of partial correlation coefficients in the typical situation when $n < p$. In particular, we consider the Moore-Penrose pseudoinverse method (PINV), the residual correlation method (RCM) and a covariance-regularized method (ℓ_{2C}). Firstly, we evaluate AUCs and timing performances on simulated datasets and we find that PINV presents some instability in AUC outcomes associated to the variable number variations. On the other hand, the two regularized methods show comparable performances with a sensible gain of time elapsing of ℓ_{2C} with respect to RCM. Finally, we present the results of an application of ℓ_{2C} for the inference of a gene network for isoprenoid pathways in *A. thaliana*. We find a negative partial correlation coefficient between HMGS and HDS, that are the two hubs in the two isoprenoid pathways. This means that they respond differently to the several tested experimental conditions and, together with the high connectivity of the two hubs, provides an evidence of cross-talk between genes in the plastidial and the cytosolic pathways. This evidence did not result from studies at level of single gene. Moreover, studies that infer this network by using only low-order partial correlation coefficients find more interactions between the two pathways with respect to the ℓ_{2C} method. A reduced number of edges between the two pathways is plausible considering the different cell compartmentalization of the two isoprenoid biosynthesis pathways.

This work was supported by grants from Regione Puglia PO FESR 2007–2013 Progetto BISIMANE (Cod. n. 44).

-
- [1] Lauritzen, S.L.: Graphical models, Oxford University Press (1996)
 - [2] Dempster, A.P.: Covariance Selection, *Biometrics* 28, 157–175 (1972)
 - [3] H. Toh H., Horimoto., K.: System for automatically inferring a genetic network from expression profiles, *J. Biol. Physics* 28, 449–464 (2002)
 - [4] Wille, A., Buhlmann, P.: Sparse graphical Gaussian modelling of the isoprenoid network in *Arabidopsis thaliana*, *Genome Biology*, 5, R92 (2004).
 - [5] Castelo, R., Roverato, A.: A robust procedure for Gaussian graphical model search from microarray data with p larger than n , *JMLR*, 7, 2621–2650 (2006)
 - [6] Gilbert, H.N., van der Laan, M.J., Dudoit, S.: Joint multiple testing procedures for graphical model selection with applications to biological networks, U.C. Berkeley Tech report, URL www.bepress.com/ucbbiostat/paper245 (2009).
 - [7] Yuan, M., Lin, Y.: Model selection and estimation in the gaussian graphical model, *Biometrika* 94, 19–35 (2007)
 - [8] Friedman, J., Hastie, T., Tibshirani R.: Sparse inverse covariance estimation with the graphical lasso, *Biostatistics* 9, 432–441 (2008)

- [9] Witten, D.M., Tibshirani, R.: Covariance-regularized regression and classification for high dimensional problems, *J. R. Statist. Soc. B* 71, 615–636 (2009)
- [10] Dobra, A., Hans, C., Jones, B., Nevins, J.R., West, M.: Sparse graphical models for exploring gene expression data, *J. Multiv. Analysis* 90, 196–212 (2004)
- [11] Schaffer, J., Strimmer, K.: An empirical Bayes approach to inferring large-scale gene association networks, *Bioinformatics* 21, 754–764 (2005)
- [12] Meinshausen N and P. Buhlmann 2006. High-dimensional graphs and variable selection with the lasso. *Ann. Statist.* 34, 1436–1462 (2006)
- [13] Friedman, J., Hastie, T., Tibshirani R.: Application of the lasso and grouped lasso to the estimation of sparse graphical models (2010)
- [14] Dijkstra, R.L.: Establishing the positive definiteness of the sample covariance matrix, *Ann. Math. Statist.* 41, 2153–2154 (1970)
- [15] Girosi, F., Jones, M., Poggio, T.: Regularization Theory and Neural Networks Architectures, *Neural Computation* 7, 219–269 (1995)
- [16] Raudys, S., Duin, R.P.W.: Expected classification error of the Fisher linear classifier with pseudoinverse covariance matrix, *Pattern Recogn. Lett.* 19, 385–392 (1998)
- [17] Disch, A., Hemmerlin, A., Bach, T.J., Rohmer, M.: Mevalonate-derived isopentenyl diphosphate is the biosynthetic precursor of ubiquinone prenyl side chain in tobacco BY-2 cells, *Biochem. J.* 331, 615–621 (1998)
- [18] Lichtenthaler, H.K., Schwender, J., Disch, A., Rohmer, M.: Biosynthesis of isoprenoids in higher plant chloroplasts proceeds via a mevalonate-independent pathway, *FEBS Lett.* 400, 271–274 (1997)
- [19] Laule, O., Frholz, A., Chang, H.S., Zhu, T., Wang, X., Heifetz, P.B., Gruissem, W., Lange, M.: Crosstalk between cytosolic and plastidial pathways of isoprenoid biosynthesis in *Arabidopsis thaliana*, *PNAS* 100, 6866–6871 (2003)
- [20] Ihmels J, Levy R, Barkai N: Principles of transcriptional control in the metabolic network of *Saccharomyces cerevisiae*. *Nat Biotechnol* 22, 86–92 (2004).